J|A|C|S
ARTICLES
Published on Web 11/27/2003

Chemical Characterization of α-Oxohydrazone Ligation on Colloids: toward Grafting Molecular Addresses onto Biological Vectors

P. Chenevier,*[,†,§] L. Bourel-Bonnet,[‡] and D. Roux[†]

Contribution from the Centre de Recherche Paul Pascal, CNRS UPR 8641, av. Pr Schweitzer, 33600 Pessac, France, and Institut de Biologie de Lille, UMR 8525, 1, rue Calmette, 59021 Lille Cedex, France

Received July 4, 2003; E-mail: pac38@cornell.edu

Abstract: New mild and specific chemical strategies have been developed recently for the selective coupling of biological macromolecules. Among them, the hydrazone ligation strategy offers high chemoselectivity and versatility. We intended to use hydrazone ligation to target the controlled release of therapeutic agents by biological vectors (multilamellar vesicles called onion vectors). An accurate measure of ligation bond stability was needed to ensure that the ligation bond would stand long exposures to physiological conditions. In this study, we have completed a kinetic and thermodynamic characterization of hydrazone formation on a model reaction. The mechanism of the reaction in solution as well as in different self-organized systems (micelles, liposomes and multilamellar vesicles) was investigated. In solution, submicromolar stability was achieved as well as half-lives of several weeks. The kinetics and stability were both enhanced in colloidal media thanks to autoassociation effects. The results were expanded to the realistic case of RGD-peptide coupling to onion vectors. The RGD grafted onion vectors were then tested for their ability to bind endothelial cells in vitro.

1. Introduction

With the recent progress in recombinant protein synthesis and chemical peptide and protein synthesis, complex macromolecules have been increasingly available for chemical modification and therapeutic uses. The manipulation of such large and delicate molecules is a new chemical challenge though and requires particular tools. Indeed, any chemical modification must be achieved in mild aqueous conditions to avoid denaturation of the macromolecule. Furthermore, for large polymers possessing multiple equivalent reactive moieties, the regioselectivity of chemical reaction has to be precisely controlled. A new series of chemical reactions addressing these requirements have been recently developed and designated as ligation reactions. Ligations can be used for large protein chemical synthesis,[1] for macromolecule coupling as in the case of immunotoxins,[2] or for grafting molecular addresses onto biological vectors.[3]

The α-oxohydrazone bond formation is well suited for this purpose. First, the reaction is done in mild aqueous conditions, and no undesirable subproduct is produced. Second, α-oxohydrazone compounds are obtained in good yields and with high chemoselectivity.[4,5] Third, the reaction is very regioselective on natural macromolecules because they contain neither hydrazine nor reactive aldehyde. Finally, the hydrazine and aldehyde moieties can be specifically designed onto synthetic as well as natural macromolecules.[6] An important question that remains concerns the kinetic and thermodynamic stability of the α-oxohydrazone bond. Indeed, hydrazones are known to hydrolyze quite easily in water, whereas ligation products such as immunotoxins or grafted vectors should be able to face extremely dilute aqueous conditions during hours if they were to be used as therapeutic agents. Fast hydrolysis is a major hurdle for using ligation in biological applications. While this question has been addressed for other systems such as disulfide bonds,[2] both the thermodynamic stability and kinetics of the α-oxohydrazone bond have to be accurately understood before it can be trusted as a good ligation strategy.

Onion vectors are multilamellar vesicles which differ from liposomes in the structure and method of preparation. Obtained by shearing of lipid lamellar phases[7] (a simple process easily scalable to industrial volumes), onion vectors can encapsulate large amounts of proteins, DNA, or organic molecules in good yields.[8] The shearing process turns the lamellar phase into a compact stack of multilamellar vesicles. Depending on the choice of lipids and surfactants, this phase can be dispersed in

[†] Centre de Recherche Paul Pascal.
[‡] Institut de Biologie de Lille.
[§] Present address: LASSP, Cornell University, Ithaca, NY 14853, USA.

(1) Nilsson, B. L.; Hondal, R. J.; Soellner, M. B.; Raines, R. T. *J. Am. Chem. Soc.* **2003**, *125*, 5268−5269.
(2) Arpicco, S.; Dosio, F.; Brusa, P.; Crosasso, P.; Cattel, L. *Bioconjugate Chem.* **1997**, *8*, 327−337.
(3) Kirpotin, D.; Park, J. W.; Hong, K.; Zalipsky, S.; Li, W.-L.; Carter, P.; Benz, C. C.; Papahadjopoulos, D. *Biochemistry* **1997**, *36*, 66−75.
(4) Melnyk, O.; Bossus, M.; David, D.; Rommens, C.; Gras-Masse, H. *J. Pept. Res.* **1998**, *52*, 180−184.
(5) Bonnet, D.; Bourel, L.; Gras-Masse, H.; Melnyk, O. *Tetrahedron Lett.* **2000**, *41*, 10003−10007.
(6) Melnyk, O.; Fehrentz, J.-A.; Martinez, J.; Gras-Masse, H. *Biopolymers* **2000**, *55*, 165−186.
(7) Diat, O.; Roux, D.; Nallet, F. *J. Phys. II France* **1993**, *3*, 1427−1452.
(8) Pott, T.; Roux, D. *FEBS Lett.* **2002**, *511*, 150−154.

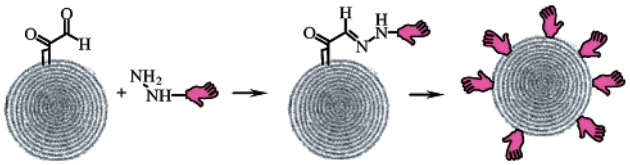

Figure 1. Grafting of ligands (hand motifs) onto onion vectors using the α-oxohydrazone ligation; transmission electron microscopy image from ref 16.

excess water. A suspension of multilamellar vesicles with concentric membranes up to the core is obtained.[9] They have proved efficient as vectors for the transport of active compounds in vivo as well as in vitro,[10,11] especially for vaccine delivery.[12,13] We have recently described their first applications as neutral targeted vectors. First, we used RGD ligands attached to a lipid moiety to ensure their association to the onion vectors.[14] The strategy was successful; however, the synthesis of the lipid−ligands proved to be delicate. Therefore, we turned to a ligation strategy, using reactive synthetic lipids in the onion vectors to graft mannose mimetic ligands in situ[15] (Figure 1). In the present study, we intend to fully understand the ligation process, so that the grafting onto onion vectors can be easily adapted to any type of ligands.

Here, we report a complete characterization of the reaction of α-oxohydrazone bond formation, in aqueous solution as well as in self-organized media. As α-oxohydrazone bonds were difficult to detect in complex media, we first studied the mechanism, kinetics, and thermodynamics of the reaction using closely related model reagents. We then used optimal conditions for the grafting of targeting ligands, RGD peptides, onto onion vectors, and tested the biological efficiency of the grafted vectors on target cells in vitro.

2. Experimental Section

2.1. Reagents and Chemicals. The buffer compounds, 3-methyl-2-benzothiazolinone hydrazone (*MBTH*) hydrochloride, dioleoyltrimethylaminomethane (*DOTAP*), and polyoxyethylene 7 lauryl ether ($C_{12}E_7$) were provided by Sigma, soybean phosphatidylcholine S100 (PC) was provided by Lipoid (France), and polyoxyethylene 8 stearoylester or Simulsol2599 (Sim) was provided by SEPPIC (France).

Hydrazinoacetyl peptides *RGDH* and *RGEH* were synthesized by solid-phase peptide synthesis, with Fmoc/*tert*-butyl standard procedures and hydrazine coupling methods developed by Bonnet et al.[17] Briefly, the YGRGDSP and YGRGESP sequences were synthesized automatically.[18] A glutaric moiety, 4,7,10-trioxa-1,13-tridecanediamine, and *N*,*N*′,*N*′-tri(*tert*-butyloxycarbonyl)hydrazinoacetic acid were coupled manually. The products were then cleaved and purified by RP-HPLC with 61% (*RGDH*) and 56% (*RGEH*) overall yield. The mass spectroscopy (TOF MS) analysis gave for *RGDH* and *RGEH* 1139.4 (MALDI) and 1156 (ESI), for calculated mass of protonated species 1139.3 and 1154.4, respectively.

Lipophilic α-oxoaldehyde (*LA*) was prepared as described previously.[19] Water soluble α-oxoaldehyde (*WA*) was kindly provided by Nathalie Ollivier: peptide SKYVL-NH_2 was prepared by automatic solid-phase peptide synthesis and oxidized by periodate oxidation.[20] Lipid−ligands *LRGD* and *LRGE* were prepared and used as described previously.[14,18]

The composition of common buffers were Tris 10 mM/EDTA 1 mM at pH 7.4 and acetic acid 100 mM at pH 4.6. Other buffers were hydrochloric (HCl 200 mM + KCl 200 mM, pH 1 to 2), citrate-phosphate (citric acid 50 mM + Na_2HPO_4 100 mM, pH 2.6 to 7), acetic (acetic acid 100 mM + NaOH, pH 3.6 to 5), carbonate (K_2CO_3 50 mM + HCl, pH 8 to 9.6), and phosphate (Na_2HPO_4 50 mM + Na_3PO_4 50 mM, pH 10 to 12) buffers.

2.2. Micelles, Liposomes, and Onion Vectors. For micelle preparations, *LA* dissolved in ethanol at 60 °C was mixed with surfactant $C_{12}E_7$ and finally dispersed in excess buffer. Final concentrations were 25 to 100 μM in *LA*, 0.25 to 1 wt % (5 to 21 mM) in $C_{12}E_7$ and less than 2% ethanol.

For liposomes and onion vectors, lipids were mixed in ethanol at 45 °C, and the ethanol was evaporated under vacuum, prior to the addition of pure water to achieve the final weight compositions: PC/Sim/water 45:20:35 for control and *LA*/PC/Sim/water 6.5:38.5:20:35 for *LA* onion vectors. Samples were incubated over half a day, before the lamellar phase was sheared between the cone tube walls and a matching cone pestle. The onion vector suspension was produced by adding a 10 time excess of pure water. For liposomes, the previous stock suspension was diluted 10 times in buffer and sonicated at high power for 10 min (10 W in 1 mL sample). Metal particles from the sonication probe were removed by a short centrifugation.

2.3. Determination of Reaction Rate Constants by Fluorometry. Rates of reaction with *MBTH* were measured by recording the fluorescence of the sample, after adding *MBTH* to a solution or colloidal suspension containing the aldehyde reagent *A* (*WA* or *LA*) to produce product *P*:

$$A + MBTH \xrightarrow{k} P + H_2O \qquad (1)$$

where k is the global reaction rate constant. The rate constant of the reverse reaction was supposed to be negligible compared to k, a hypothesis justified by the high stability of *P*. Fluorescence intensity was measured in a thermostated 5 mm square quartz cuvette, using a Fluoromax (Spex, USA) fluorometer. The fluorescence intensity (excitation 366 nm, emission 495 nm) was linear in the concentration of *P* up to 60 μM and 100 μM for the products of reaction of *MBTH* with *WA* and *LA*, respectively (data no shown). Fluorescence intensity time series were then fitted to the second-order reaction rate equation:

$$IF = IF_0 + IF_{\max}\frac{1 - e^{-t/\tau}}{1 - (a/n)e^{-t/\tau}} \qquad (2)$$

where $\tau = k^{-1}(n - a)^{-1}$, IF, IF_0, and $IF_{\max}$ are the recorded instantaneous, initial, and final fluorescence intensities, respectively, and a and n, the initial global concentrations of *A* and *MBTH* (τ, IF_0, and $IF_{\max}$ were the adjustable parameters). k was determined from several values of τ measured with different values of n and a. Concentrations ranged typically from 200 μM to 2 mM for *MBTH* and between 5 and 100 μM for α-oxoadehydes.

Concentrations of nonprotonated hydrazines vary with pH so that global rate constants cannot be directly compared at different pHs. For varying pHs, the global rate constant k was corrected into k_{corr} as

(9) Gulik-Krzywicki, T.; Dedieu, J. C.; Roux, D.; Degert, C.; Laversanne, R. *Langmuir* **1996**, *12*, 4668−4671.
(10) Freund, O.; Amédée, J.; Roux, D.; Laversanne, R. *Life Sci.* **2000**, *67*, 411−419.
(11) Mignet, N.; Brun, A.; Degert, C.; Delord, B.; Hélène, C.; Laversanne, R.; François, J.-C. *Nucleic Acids Res.* **2000**, *28*, 3134−3142.
(12) Gaubert, S. World Patent WO99/16468, 1998.
(13) Gaubert, S. World Patent WO01/19335A2, 2001.
(14) Chenevier, P.; Delord, B.; Amédée, J.; Bareille, R.; Ichas, F.; Roux, D. *Biochim. Biophys. Acta* **2002**, *1593*, 17−27.
(15) Chenevier, P.; Grandjean, C.; Loing, E.; Malingue, F.; Angyalosi, G.; Gras-Masse, H.; Roux, D.; Melnyk, O.; Bourel-Bonnet, L. *Chem. Commun.* **2002**, *20*, 2446−2447.
(16) Roux, D.; Chenevier, P.; Pott, T.; Navailles, L.; Regev, O.; Mondain Monval, O. *Curr. Med. Chem.*, to be published.
(17) Bonnet, D.; Grandjean, C.; Rousselot-Pailley, P.; Joly, P.; Bourel-Bonnet, L.; Santraine, V.; Gras-Masse, H.; Melnyk, O. *J. Org. Chem.* **2003**, *68*, 7033−7040.
(18) See Supporting Information for details.
(19) Bourel-Bonnet, L.; Gras-Masse, H.; Melnyk, O. *Tetrahedron Lett.* **2001**, *42*, 6851−6853.
(20) Georgheran, K. F.; Stroh, J. G. *Bioconjugate Chem.* **1992**, *3*, 138−146.

described by Sayer et al.:[21,22]

$$\frac{k_{corr}}{k} = \frac{K'_a + [H^+]}{K'_a} \quad (3)$$

where K'_a is the protonation constant of the *MBTH*.

2.4. Determination of Thermodynamic Equilibrium Constants. Stoichiometric mixtures of aldehyde and hydrazine reagents were prepared at different concentrations, *n*, and reacted for 24 h at room temperature. The fluorescence intensity (or alternatively UV absorption at 250−275 nm for solutions) of the samples was measured. The product concentration, *p*, depended on the equilibrium constant, *K*, and on *n* as $p = n + (K^{-1}/2) - \sqrt{(K^{-1}/n)+(K^{-2}/4)}$). As *K* was large, *p* was nearly equal to *n*. To highlight the slight gap, the relative fluorescence intensity was plotted versus concentration *n* as $p/p_{max} - n/n_{max}$ and fitted to equation below:

$$p/p_{max} - n/n_{max} = M\frac{n + \frac{1}{2K} - \sqrt{\frac{1}{nK} + \frac{1}{4K^2}}}{n_{max} + \frac{1}{2K} - \sqrt{\frac{1}{n_{max}K} + \frac{1}{4K^2}}} - \frac{n}{n_{max}} \quad (4)$$

where p_{max} and n_{max} refer to the sample of highest concentration, and *M* and *K* are the adjustable parameters (*M* accounts for experimental errors on n_{max} and p_{max} and was always close to 1). Equilibrium constants were measured at low pH where hydrazines are protonated. The apparent constant K_{app} was deduced from eq 4, and the real equilibrium constant was deduced as for rate constants: $K = K_{app}(K'_a + [H^+])/K'_a$.

2.5. Acidity and Phase Transfer Constants of *MBTH*. The protonation constant of *MBTH* was measured as the pH of buffer solutions (i.e., containing 50% of the base and 50% of the protonated form) of *MBTH* at different concentrations. n_M moles of *MBTH* hydrochloride were placed in a vial and diluted to the desired concentration. The pH was measured under stirring while $n_M/2$ mol of sodium hydroxide were added. The pH of buffer solutions of concentrations 20, 10, 5, and 2.5 mM were 5.66, 5.67, 5.66, and 5.70, respectively, giving the pK'_a value with good accuracy: $pK'_a = 5.67$ at 25 °C.

The phase transfer equilibrium constant K_{pt} of *MBTH* between water and lipid colloids was estimated in liposome suspensions. It is defined as $K_{pt} = [MBTH]_{lip}/[MBTH]_{wat}$ where subscripts "lip" and "wat" refer to concentrations in the lipid phase and the water phase volumes, respectively. Control liposomes were prepared in buffers at pH 4.6, 7.7, and 3.8. Different dilutions of liposomes (0.15 to 15 g/L lipids) were incubated with 200 μM *MBTH* for 24 h at room temperature in the dark. Liposomes were then removed by ultrafiltration (Microcon centrifugal filters, Millipore, USA), and the concentration of *MBTH* in the bulk was measured by UV absorption. K_{pt} was deduced by fitting the following equation to the data:

$$[MBTH]/[MBTH]_{wat} = 1 + K_{pt}C\bar{v} \quad (5)$$

where [*MBTH*] is the initial global concentration of *MBTH* in the suspension and $C\bar{v}$ is the volume fraction of the lipid phase (considered negligible compared to the water volume). $C\bar{v}$ was estimated as half of the volume of lipids in the suspension (see below). The measurement ($K_{pt} = 600 \pm 350$) was not very accurate because the separation of liposomes by ultrafiltration was incomplete. The same experiment using onion vectors separated by centrifugation gave similar but less accurate results.

(21) Sayer, J. M.; Peskin, M.; Jencks, W. P. *J. Am. Chem. Soc.* **1973**, *95*, 4277−4287.
(22) Sayer, J. M.; Pinsky, B.; Schonbrunn, A.; Washtien, W. *J. Am. Chem. Soc.* **1974**, *96*, 7998−8009.

2.6. Detection of *RGDH* Ligation Product by Mass Spectroscopy. *LA* or control onion vectors (6.5 g/L lipids, ∼85 μM accessible aldehydes; see calculation below) were incubated for 24 h with *RGDH* (170 μM) at pH 5.0 (acetic buffer 10 mM). They were centrifuged (3 h, 4 °C, 26 000 × *g*), dispersed in buffer and centrifuged again twice to eliminate excess *RGDH*. Onion vectors were dispersed in water and dissolved by adding 2 volumes of ethanol for immediate analysis by MALDI-TOF MS (Voyager-DE PerSeptive Biosystems, USA) in acid α-cyano-4-hydroxycinnamic matrix.

2.7. Cell Adhesion Tests. For cell adhesion tests, onion vectors were prepared as described earlier[14] with the following lipid weight compositions: PC/MO 95:5 for control and marker lipid/PC/MO 10:85:5 for labeled onion vectors, where the marker lipid were *LA*, *LRGD*, *LRGE*, and *DOTAP* for *LA*, RGD, RGE, and cationic vectors, respectively. Lipid mixes were treated as described above, except that they were hydrated with a solution of calcein (1 mM, pH 5.6) instead of water in a 48:52 water/lipids weight ratio. *LA* vector stock suspensions were diluted 10 times in buffer pH 4.6 (acetate 10 mM) and incubated for 4 h with 100 μM *RGDH* or *RGEH* at room temperature in the dark. Onion vectors were then centrifuged (30 min, 4 °C, 11 000 × *g*) and resuspended in phosphate buffer pH 7.4.

Cell adhesion tests were performed as described earlier.[14] Briefly, endothelial cells of the EAhy-926 cell line[23] were harvested using trypsin, washed thoroughly, mixed with onion vectors, centrifuged shortly (5 min, 4 °C, 400 × *g*), and incubated for 4 h at 37 °C in a CO_2 enriched atmosphere. Excess onion vectors were carefully washed out, cells were harvested with a pipet, and propidium iodide was added (PI, 0.5 μg/mL) for immediate analysis by flow cytometry (FACScan, Becton-Dickinson). The relative intrinsic fluorescences *q* of onion vector suspensions were measured independently by fluorometry in the presence of cobalt(II) chloride (Co^{2+} ions quench the fluorescence of nonencapsulated calcein, which amounts to 5−40% of total calcein). The average cell fluorescence of live cells *FC* was calculated as the median of the PI-negative data and corrected for intrinsic onion vector fluorescence as $FC_{corr} = (FC - FC_{untreated})/q$, where $FC_{untreated}$ refers to the fluorescence of cells treated with no onion vectors.

3. Results

Before preparing and testing grafted vectors as presented in Figure 1, we studied the reaction of grafting in a more general case:

$$RR'N{-}NH_2 + R''CO{-}CHO \xrightarrow{k,K} RR'N{-}N{=}CH{-}COR'' + H_2O \quad (6)$$

where *k* is the global rate constant, and *K*, the global equilibrium constant of the reaction. The reaction mechanism was first investigated in water, using the water soluble aldehyde *WA* (Figure 2) and *N*-methylbenzothiazolinone hydrazone (*MBTH*) as model reagents. Second, the effect of self-organized colloidal media on the reaction was studied, in micelles, liposomes, or onion vectors suspensions. We compared the reaction kinetics and thermodynamics in two cases: (i) the reaction takes place mainly in the water bulk (using aldehyde *WA*) in the presence of non reactive colloids, and (ii) the reaction takes place mainly at the surface of colloids where the lipophilic aldehyde (*LA*) is sequestered. Third, the results obtained with the model reagent *MBTH* were extended to peptidic hydrazines. Finally, the grafting of peptide ligands onto onion vectors using the α-oxohydrazone ligation was optimized and tested on cultured cells.

(23) Edgell, C. J. S.; McDonald, C. C.; Graham, J. B. *Proc. Natl. Acad. Sci. U.S.A.* **1983**, *80*, 3734−3737.

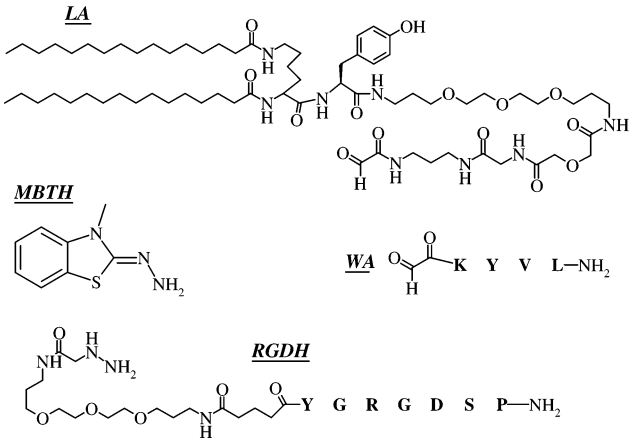

Figure 2. Structures of α-oxoaldehyde and hydrazine reagents; amino acids are represented in the one letter code as bold letters.

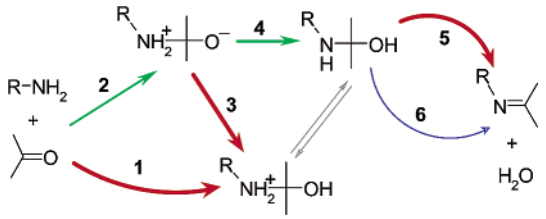

Figure 3. Mechanistic model for imine formation according to Sayer et al.[22] The rate determining steps are indicated by single arrows; noncatalyzed (2 and 4), acid catalyzed (1, 3, and 5), and base catalyzed (6) steps are shown as green, red, and blue arrows, respectively.

Although α-oxohydrazone bonds can be detected by UV absorption, they are difficult to trace in solutions containing proteins, peptides, or lipid vesicles, which absorb UV light. Therefore, we turned to a model reaction that could be monitored as well in peptidic solution as in turbid media. The molecular address hydrazine was replaced by the fluorescent probe *MBTH*, which becomes fluorescent when its hydrazine moiety is involved in a hydrazone bond. *MBTH* was reacted with *WA* or *LA*, giving the respective reaction products *WP* and *LP*.

3.1. Kinetics in Solution According to Sayer's Mechanistic Model. The general mechanism of imine and hydrazone formation in aqueous solution has been thoroughly described by Sayer et al.,[21,22,24] as summarized in Figure 3. It shows the addition of a nucleophile amine on a carbonyl compound to form a hydroxylamine, followed by the dehydration of the hydroxylamine into an imine. Some or all of the mechanistic steps can be successively rate determining when changing the pH of the solution. According to this model, in the case of a strong nucleophile and a very electrophilic carbonyl, such as hydrazine and α-oxoaldehyde used in our study, all 6 steps should be successively rate determining, allowing the determination of all mechanistic rate constants.

Referring to Sayer's model, we investigated the reaction of *MBTH* with *WA* in solution as a function of pH. Fluorescence time series were analyzed according to eq 6 and showed a first-order kinetics toward each reagent. The global reaction rates k as a function of pH (Figure 4, triangles) depend both on the rate determining step and on the protonation of hydrazine into unreactive hydrazonium. As described by Sayer et al., we measured the pK_a of *MBTH* (pK_a = 5.67 in water at 25 °C)

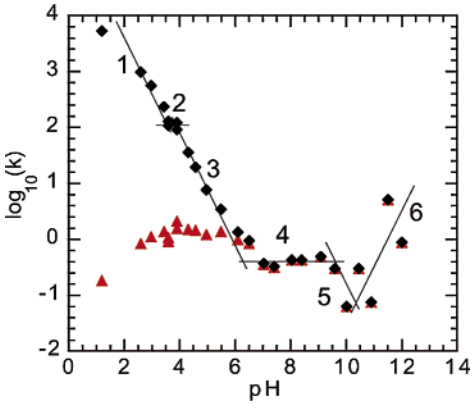

Figure 4. Logarithm of rate constant log(k) of hydrazone formation as a function of pH, for the reaction of *MBTH* with *WA* at 25 °C. (▲) Observed rate constants; (◆) rate constants corrected for hydrazine concentration. Numbers refer to the mechanistic model of Sayer et al. (Figure 3).

Table 1. Rate Constants of Rate Determining Steps for the Reaction of *MBTH* with *WA* at 25 °C, as Measured in Figure 4

measured rate[i]	constant	literature data
k_1 (M^{-2} s^{-1})	4.3×10^5	<5800[a,c]
k_2 (M^{-1} s^{-1})	100	≈1000[a,b]
K_2k_3 (M^{-2} s^{-1})	8.1×10^5	$<2 \times 10^5$ [h]
K_2k_4 (M^{-1} s^{-1})	0.36	0.001[d]−85[h]
$K_2K_4k_5$ (M^{-2} s^{-1})	2×10^9	$<1.8 \times 10^6$ [f]
$K_2K_4k_6$ (M^{-2} s^{-1})	300	0.3[g]−7×10^5[e]

[a] Literature data: reaction at 25 °C of *p*-chlorobenzaldehyde with phenylhydrazine-*p*-sulfonate. [b] Literature data: reaction at 25 °C of *p*-chlorobenzaldehyde with methoxyamine [c] Literature data: reaction at 25 °C of *p*-chlorobenzaldehyde with hydroxylamine [d] Literature data: reaction at 25 °C of *p*-chlorobenzaldehyde with 2-methyl-3-thiosemicarbazide.[22] [e] Literature data: reaction at 25 °C of *p*-chlorobenzaldehyde with *N*-aminoyridinium chloride. [f] Literature data: reaction at 25 °C of *p*-chlorobenzaldehyde with hydrazine. [g] Literature data: reaction at 25 °C of *p*-chlorobenzaldehyde with semicarbazide.[21] [h] Literature data: reaction at 25 °C of *p*-methoxybenzaldehyde with methoxyamine.[24] [i] Indices of rate and equilibrium constants (noted k and K, respectively) refer to steps in the mechanistic model of Sayer et al. (Figure 3).

and corrected the rate constant for actual hydrazine concentration at each pH (Figure 4, diamonds). Depending on pH, the corrected rate constant was either constant or varied linearly with proton concentration, highlighting changes in the rate determining step. As predicted by Sayer's model, the six steps depicted in Figure 3 were successively rate determining from pH 1 to 13; although the plateau corresponding to step 2 was very small on the pH corrected curve (diamonds Figure 4), it was evidenced by the discontinuity in the noncorrected curve around pH 4 (triangles). As shown in Table 1, the values of each step's rate constants compared well with previously published data for the reaction of electrophilic aldehydes and strong nitrogen nucleophiles.[21,22,24−27] However, the rate constants of the acid catalyzed steps (1, 3, 5 in Figure 3) were unexpectedly high: they were far higher than equivalent rate constants in reactions involving very strong reagents as hydrazine, hydroxylamine, or methoxyamine.

As the rate of formation of the hydrazone was optimal in mild acidic solutions, the pH 4.6 was chosen as the optimal pH for further experiments.

(24) Rosenberg, S.; Silver, S. M.; Sayer, J. M.; Jencks, W. P. *J. Am. Chem. Soc.* **1974**, *96*, 7986−7998.
(25) Sayer, J. M.; Jencks, W. P. *J. Am. Chem. Soc.* **1977**, *99*, 464−474.
(26) Hine, J.; Via, F. A.; Gotkis, J. K.; Craig, J. C. *J. Am. Chem. Soc.* **1970**, *92*, 5186−5193.
(27) Hine, J.; Cholod, M. S.; Chess, W. K. *J. Am. Chem. Soc.* **1973**, *95*, 4270−4276.

Table 2. Measured Rate Constants *k* and Equilibrium Constants *K* for the Reaction of *MBTH* with *WA* or *LA* at 25 °C in Different Aqueous Media[a]

	medium	k (M^{-1} s^{-1}) at pH 4.6	k (M^{-1} s^{-1}) at pH 7.4	K ($\times 10^6$ M^{-1})	k_{hyd} (s^{-1}) at pH 7.4
WA	buffer	1.33 ± 0.15	0.29 ± 0.07	0.53 ± 0.07	5×10^{-7}
	micelles 1%	2.0 ± 0.3	0.70 ± 0.03	1.9 ± 0.6	4×10^{-7}
	liposomes	1.3	ND	ND	ND
LA	micelles 0.25%	7.3 ± 0.5	ND	ND	ND
	micelles 1%	2.4 ± 0.2	1.5 ± 0.1	97 ± 89	1.5×10^{-8}
	liposomes or onion vectors	5.1 ± 0.9	1.5 ± 0.3	15 ± 5	10^{-7}

[a] k_{hyd}: rate constant of hydrolysis. ND: not determined.

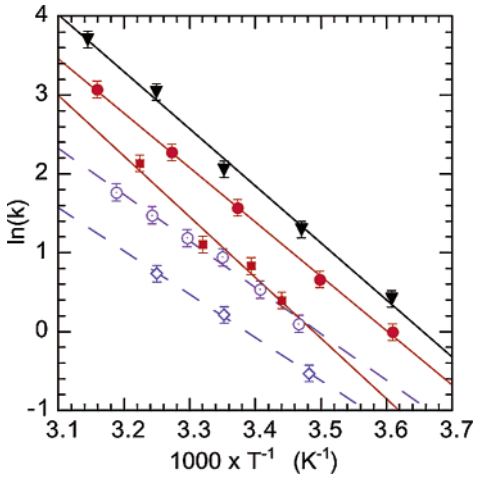

Figure 5. Reaction rates *k* of *LA* or *WA* with *MBTH* at pH 4.6 as a function of the reciprocal temperature. (Open symbols) *WA* in solution (○) or in micellar suspension 1% $C_{12}E_7$ (◇); (closed symbols) *LA* in micellar suspension 0.25% $C_{12}E_7$ (●) or 1% $C_{12}E_7$ (■) and in liposome suspension (▼). Lines are best fits of the Arrhenius equation $\ln(k) = \ln(A) - E_a/RT$.

3.2. Kinetics in Colloidal Suspension. We then compared the reactivity of *MBTH* with α-oxoaldehydes in different media at optimal and physiological pH. Reaction rates with the lipophilic reagent *LA* inserted into lipidic colloids (micelles, liposomes and onion vectors) were compared to reaction rates with the water soluble reagent *WA* in buffer or in colloidal suspension (Table 2). Reaction rates of bond formation were found to increase up to a factor of 5 in the presence of colloids. The increase was always small in the case of the reaction of *MBTH* with *WA* but could be high for reactions with *LA* embedded in colloids. Considering the Arrhenius model $k = A \exp(-E_a/RT)$, an increase in *k* can be due either to a reduced activation energy, E_a, or to an increase in the prefactor, *A*. The former would derive from a catalysis of the reaction, while the later would emphasize inhomogeneities in the reaction medium. To distinguish between these hypotheses, the dependence of rate constants on temperature was investigated.

3.3. Temperature Dependence of Rate Constants. The rate constants of the reaction of *MBTH* with *LA* or *WA* was measured as a function of temperature at the optimal pH. They are reported in an Arrhenius plot in Figure 5. The corresponding activation energies and prefactors are given in Table 3. Studying the temperature dependence of reactions in complex media is not an easy task, as the complex solvent changes with temperature. As a consequence, activation parameters might contain contributions from these structural changes. However, our complex media showed little variation in their physical properties over the range of temperatures and concentrations used. In particular, $C_{12}E_7$ at 0.25% and 1% between 5 and 45 °C is well above its critical micellar concentration and forms small micelles.[28,29] We therefore considered the measured activation parameters as mainly driven by the chemical reaction itself.

Table 3. Activation Energies E_a and Arrhenius Prefactors *A* for the Reaction of *WA* or *LA* with *MBTH* at pH 4.6, as Determined in Figure 5

	medium	E_a (kJ/mol)	ln(*A*)
WA	buffer	49 ± 5	20.6 ± 1.7
	micelles 1%	45 ± 7	18.5 ± 2.5
	micelles 0.25%	57 ± 3	24.8 ± 1.2
LA	micelles 1%	64 ± 6	26.9 ± 1.5
	liposomes	60 ± 3	26.4 ± 1

Contrary to what was expected from its higher rate constant, the reaction of *LA* with *MBTH* had a higher activation energy than that of *WA*. Furthermore, within experimental errors, activation energies depended only on the reagents and not significantly on the reaction medium. We conclude that the mechanism of the reaction was not deeply changed in the presence of colloids and colloids had no catalytic effect. The gap in activation energy between *LA* and *WA* is not understood but could be due to their structural differences, such as the protonated lysine in *WA* which could act as an intramolecular catalyst.

The reaction rate was mostly increased by changes in the frequency of reagents encounter, accounted for by the Arrhenius prefactor *A*. It is worth noting that *A* should decrease when one of the reagents is immobilized on a colloid. Indeed, the Brownian motion of the immobilized molecule is considerably reduced compared to a free molecule in solution. Furthermore, the immobilized molecule can only be approached from a half space defined by the colloidal surface, whereas free molecules in solution can be approached from all directions (see Shield et al. for complete calculations[30]). Therefore, *A* can increase only if both reagents have inhomogeneous concentrations in the colloidal media and concentrate in the same place.

3.4. Partition of Reagents and Products in Different Phases of Colloidal Media. We investigated possible reagent adsorption on colloids that could account for their inhomogeneous concentrations in colloidal media. *LA* as well as *LP* partitioned only in lipidic colloids because of their two aliphatic chains (100% of *LP* fluorescence was found in the colloids after separation by centrifugation). As a contrary, *WA* was supposed to be mostly hydrophilic because of its zwitterionic charge and hydrophilic tail, whereas the aromatic *MBTH* is known to be partly

(28) Constantin, D.; Freyssingeas, E.; Palierne, J.-F.; Oswald, P. *Langmuir* **2003**, *19*, 2554−2559.
(29) Sharma, K. S.; Patil, S. R.; Rakshit, A. K. *Colloids Surf., A* **2003**, *219*, 67−74.
(30) Shield, S. R.; Harris, J. M. *J. Phys. Chem. B* **2000**, *104*, 8527−8535.

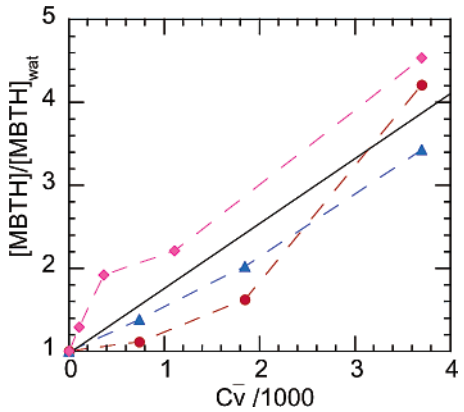

Figure 6. Determination of *MBTH* partition constant between liposomes and water at pH 7.7 (●), 3.8 (▲), and 4.6 (◆) at 25 °C; the continuous line is the best fit to all data of eq 5.

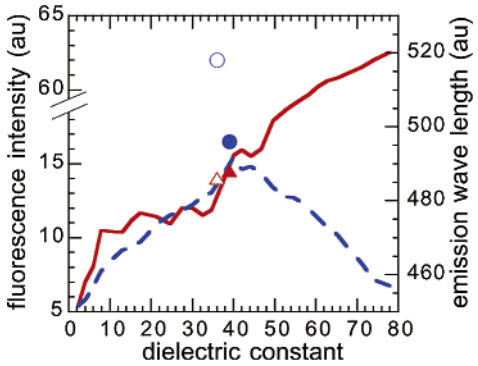

Figure 7. Maximum emission wavelength (continuous line) and fluorescence intensity (dashed line) of the product of reaction of *MBTH* with *WA* as a function of dielectric constant in water/dioxane mixtures at 25 °C; maximum emission wavelength (triangles) and fluorescence intensity (circles) of *WP* (closed symbols) or *LP* (open symbols) in micellar suspension (1% $C_{12}E_7$).

hydrophobic (its nonprotonated form is insoluble above 5 mM in water). However, the partition constants of *WA* and *MBTH* were too low to be measured accurately. Only for *MBTH* could the partition constant K_{pt} between liposomes and water be roughly estimated to $K_{pt} = 600 \pm 350$ (Figure 6). Surprisingly, no strong dependence on pH was observed. The accuracy of measurement was limited by the small fraction of liposomes that could not be filtered out and induced a strong UV light scattering. The result was also strongly dependent on the estimation of the volume fraction of the lipid phase, $C\bar{v}$, in which *MBTH* dissolved. $C\bar{v}$ could not be measured independently; it was assumed to be half of the total lipid volume in liposomes (see below).

Adsorption of fluorescent products was also indicated by changes in emission spectra in the presence of colloids. The fluorescent product *WP* had a quantum yield of 10^{-4} with a wavelength of maximal emission $\lambda_{max} = 520$ nm in buffer at pH 4.6 or 7.4 and 25 °C. In micellar solution (1%), its quantum yield increased to 5×10^{-4} with a blue shift to $\lambda_{max} = 488$ nm. For comparison, the fluorescence of *WP* was measured in mixtures of water and dioxane (Figure 7), whose dielectric constants can vary from 78 in pure water to 2 in pure dioxane, mimicking all environments from the aqueous bulk to the inner core of micelles.[31] As the dioxane volume fraction increased

(31) Lakowicz, J. R. *Principles of Fluorescence Spectroscopy*; Plenum Press: 1983.

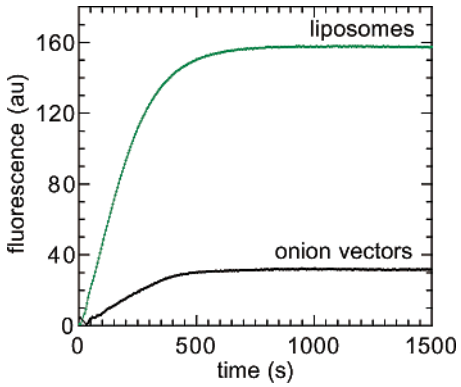

Figure 8. Kinetics of reaction of *MBTH* (1 mM) with *LA* (104 μM) inserted into liposomes or onion vectors (1.3 g/L lipids) of the same composition, at pH 4.6 and 25 °C.

from 0 to 1, a progressive blue shift from 520 to 452 nm was observed. Fluorescence characteristics similar to those of *WP* and *LP* in colloidal media (i.e., a high fluorescence intensity and λ_{max} near 488 nm) were recorded for mixtures of dioxane with the volume fraction near 0.5 and dielectric constant $\epsilon \approx 40$, corresponding to an environment of intermediate lipophilicity. This indicated that the fluorochrome part of *WP* and *LP* adsorbed at the surface of micelles but did not penetrate deeply into the lipophilic core.

3.5. Effect of Structural Complexity of Colloids: Liposomes versus Onion Vectors. Assuming a homogeneous repartition in the membranes, *LA* in liposomes and onion vectors was shared in two different classes regarding accessibility to reagents in the bulk water phase: *LA* molecules displayed on the surface were directly exposed, whereas those embedded in inner monolayers were protected from the bulk by at least one lipid bilayer. To investigate the reactivity of each class, the reaction yield was compared for reactions of *MBTH* with *LA* onion vectors and liposomes. Both colloids had the same chemical composition, as liposomes were obtained by high power sonication of the onion vectors. Although the concentration and chemical environment of *LA* were strictly identical, the reaction yield was expected to depend on the proportions f_{ov} and f_{lip} of surface exposed *LA* in onion vectors and liposomes, respectively. As shown by AFM imaging of the suspensions, the onion vector preparations were composed of 72%/28% onion particles/unilamellar vesicles (% in number), whereas the liposome preparations were reduced to mostly unilamellar vesicles with 96%/4% unilamellar vesicles/onion particles (data from J. Thimonier and J. Barbet, not shown). Onion vectors were made of concentric lipid bilayers of thickness δ, stacked regularly from the center to the surface with a constant spacing d.[8,9] We assumed that *LA* was dispersed statistically into all monolayers, so that f_{ov} was equal to the volume ratio of the outermost monolayer v_{om} and the total lipid volume of an onion vector v_{tot}. We obtain $f_{ov} = v_{om}/v_{tot} = d/\delta(1 - (1 - \delta/2r)^3) \approx 3d/2r$, where r is the average radius of onion vectors. For our onion vectors, d was measured to 70 Å by X-ray diffraction,[8] and r, to 100 nm by static and dynamic light scattering (data not shown), so that $f_{ov} \approx 0.1$. As for liposomes, they were made of one bilayer containing roughly half of the lipids on each monolayer, so that $f_{lip} \approx 0.5$.

Fluorescence monitorings are reported in Figure 8. The yield of reaction was 5 times lower with onion vectors than with liposomes, a ratio close to the ratio of surface exposed *LA*

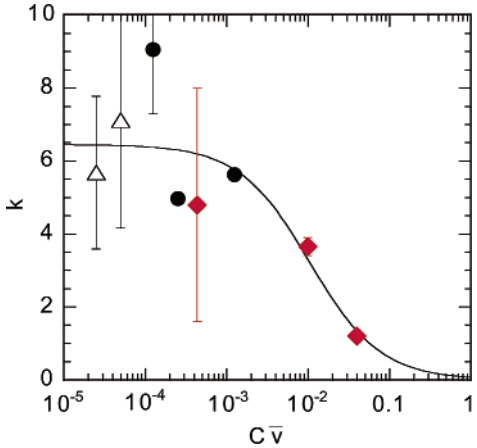

Figure 9. Apparent reaction rate constant *k* of *LA* with *MBTH* as a function of pseudophase volume fraction $C\bar{v}$ at pH 4.6 and 25 °C: (△) in onion vector suspension; (●) in liposome suspensions; (◆) in micellar suspensions. The curve corresponds to the best fit of eq 9.

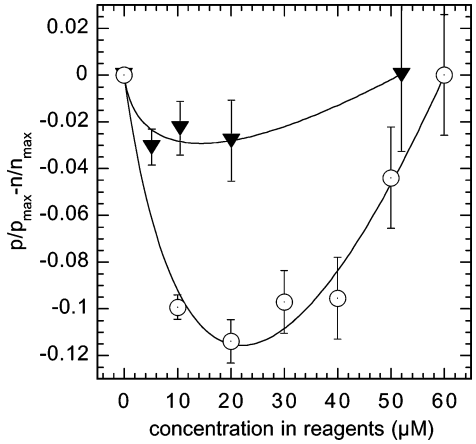

Figure 10. Determination of equilibrium constant *K* for the reaction of *LA* in liposomes (▼) or *WA* in solution (○) with *MBTH* at pH 4.6 and 25 °C. The lines are the best fit of eq 4 to the measured gap to linearity $p/p_{max} - n/n_{max}$ (see Experimental Section).

concentration f_{lip}/f_{ov}. This indicates that only surface exposed *LA* had reacted. Then, it seems that *MBTH* adsorbed but did not cross bilayers in the time course of our experiments. This relates well with the low lipophilicity of *MBTH* and *MBTH* hydrazone products as noted above.

3.6. Reaction Rate Dependence on Accessible Lipid Concentration. The observed rate changes in the reaction of *MBTH* with *LA* were then analyzed in the following pseudophase model. The reaction was supposed to occur only in the lipidic pseudophase, where *LA* was completely sequestered, and its rate was modulated by the partition of *MBTH* between the two phases:

$$MBTH_{wat} \overset{K_{pt}}{\rightleftharpoons} MBTH_{lip} \tag{7}$$

$$MBTH_{lip} + LA_{lip} \overset{k_{lip},\, K_{lip}}{\rightleftharpoons} LP_{lip} \tag{8}$$

where k_{lip} and K_{lip} are the reaction rate and equilibrium constants in the pseudophase and subscripts "wat" and "lip" refer to solutes in the bulk water phase and the lipidic pseudophase, respectively. Assuming a rapid partition equilibrium compared to hydrazone formation, the apparent rate constant *k* could be derived as

$$k = \frac{k_{lip} K_{pt}}{1 + K_{pt} C\bar{v}} \tag{9}$$

where $C\bar{v}$ is the volume fraction of pseudophase in the suspension, *C* is the global concentration of lipids constituting the pseudophase, and $\bar{v}$ is the specific volume of those lipids. As *MBTH* did not penetrate into complex lipid colloids during the time scale of the reaction, only the accessible lipids in the outermost monolayer were considered to take part to the pseudophase. $\bar{v}$ was estimated from the molecular mass of the corresponding lipids, as their density is very close to 1 ($\bar{v} \approx 0.5$ for micelles, $\bar{v} \approx 0.8$ for liposomes and onion vectors). Figure 9 shows the variations of the global rate constant *k* with $C\bar{v}$.

Within experimental error, the model fitted well the data and gave values of $K_{pt} = 95 \pm 50$ and $k_{lip} = 0.1 \pm 0.05$ M^{-1} s^{-1}. K_{pt} was lower but still in reasonable agreement with the partition constant estimated above to $K_{pt} = 600 \pm 350$. The rate constant k_{lip} of bond formation in the lipidic pseudophase was significantly reduced compared to the rate constant measured in aqueous solution with *WA* and *MBTH*. This confirmed that the reaction of *MBTH* with *LA* was locally slower, as the higher activation energy suggested. Only the high concentration of both reagents near the colloids due to lipophilic adsorption accounts for the increase in global reaction rate.

In the case of the reaction of *WA* with *MBTH*, the reaction very probably takes place in both phases simultaneously. The effect on the reaction kinetics is low though, and the low accuracy of our measurement did not allow us to identify the role of each phase in the reaction kinetics.

3.7. Hydrazone Bond Stability. Both the thermodynamic and kinetic aspects of α-oxohydrazone bond stability were investigated. We measured first the equilibrium constant *K* and then the reaction rate constant *k* at pH 7.4 to deduce the rate of hydrolysis k_{hyd} at physiological pH as $k_{hyd} = k/K$. The equilibrium constants *K* were determined by measuring the yield of reaction at equilibrium as a function of reagent concentrations (Figure 10). As *K* was quite high, it was measured at acidic pH where competition with hydrazine protonation reduced the apparent equilibrium constants to detectable values. The equilibrium constants *K* deduced from these measures are reported in Table 2. They were found to be very high compared to other imines or hydrazones. Indeed, reported equilibrium constants *K* for the formation of imines and hydrazones in water at 25 °C are at the most in the micromolar range: the most stable imines are in the millimolar range, whereas the best hydrazones (*p*-chlorobenzaldehyde/*p*-toluenesulfonylhydrazine, $K = 2.4 \times 10^4$ M^{-1} or *p*-chlorobenzaldehyde/semicarbazide, $K = 5.5 \times 10^5$ M^{-1} [26,24]) and oximes (protonated 2-quinolinecarboxaldehyde/hydroxylamine, $K = 1.27 \times 10^5$ M^{-1} [32]) access the micromolar range.

Apparent equilibrium constants for *LP* were higher than those for *WP*, as expected in the pseudophase model. Indeed, partition of the reagents and products into the small volume of the pseudophase should increase strongly their local concentrations and favor bond formation. In the model eqs 7 and 8, the global equilibrium constant *K* depends on the partition constant K_{pt} of *MBTH* and on the local equilibrium constant K_{lip} in the

(32) Malpica, A.; Calzadilla, M. *J. Phys. Org. Chem.* **2003**, *16*, 202−204.

Table 4. Measured Rate Constants *k* at pH 4.6 and Equilibrium Constant *K* for the Reaction of *RGDH* and *MBTH* with *WA* or *LA* at 25 °C in Solution or Liposome Suspension

	WA/buffer		*LA* liposomes	
	k ($M^{-1}s^{-1}$)	*K* ($10^6\ M^{-1}$)	*k* ($M^{-1}s^{-1}$)	*K* ($10^6\ M^{-1}$)
MBTH	1.33 ± 0.15	0.53 ± 0.07	5.6 ± 0.5[a]	15 ± 5
RGDH	0.53	47 ± 20	0.9 ± 0.6[a]	ND[b]

[a] Determined with competition reaction experiments. [b] ND: not determined.

pseudophase as $K = K_{lip}K_{pt}/(1 + K_{pt}C\bar{v})$. Taking into account the small volume fraction of lipids, $C\bar{v}$, in most of our colloidal preparations and the relatively high partition constant K_{pt}, we expect an increase in global equilibrium constant *K* of about 2 orders of magnitude between the reaction in water and at the surface of colloids. This is in fairly good agreement with our data in Table 2.

3.8. Grafting of Targeting Peptides onto Biological Vectors. We applied the results of our study on the model reaction to a real application: grafting of RGD peptides as molecular addresses onto onion vectors. We first compared the reactivity of the peptide hydrazine *RGDH* with that of *MBTH* to check how far the results obtained with *MBTH* could be extended to peptide hydrazines. The reaction rate *k* at pH 4.6 and equilibrium constant *K* of the reaction of *RGDH* and *WA* were measured in solution as previously described for *MBTH*, using UV absorption measurement (250−275 nm) instead of fluorometry (Table 4).

Reaction rates on colloids could not be measured by the same procedure though, as colloidal media absorb most of the UV light. They were evaluated by an indirect measure: a competition reaction. *LA* was reacted simultaneously with *MBTH* and *RGDH* to give products *LP* and *LRGDH* at rate constants k_{MBTH} and k_{RGDH}, respectively:

$$LA + MBTH \xrightarrow{k_{MBTH}} LP + H_2O$$

$$LA + RGDH \xrightarrow{k_{RGDH}} LRGDH + H_2O \qquad (10)$$

Only the apparition of *LP* was observed (Figure 11), but it was slowed and limited by the consumption of *LA* reacting with *RGDH*. The reaction kinetics was modeled by the following equation system:

$$\frac{dp}{dt} = k_{MBTH}(n - p)(a - p - p')$$

$$\frac{dp'}{dt} = k_{RGDH}(n' - p')(a - p - p') \qquad (11)$$

where *p* and *p*′ are the respective instantaneous concentrations of *LP* and *LRGDH*, and *n*, *n*′, and *a*, the respective initial concentrations of *MBTH*, *RGDH*, and accessible *LA*. Equations 11 can be solved numerically. The calculated *p* curve was fitted to fluorescence data to determine the rate constants (continuous line in Figure 11) from which the reactivity of *RGDH* was deduced (dashed line). Rate constants are presented in Table 4.

The formation of *LRGDH* on onion vectors was evidenced by mass spectroscopy. After incubation of *LA* or control onion vectors with or without *RGDH*, the vectors were washed and dissolved in ethanol for immediate analysis by MALDI-TOF MS (data not shown). *LRGDH* was detected only in the case of

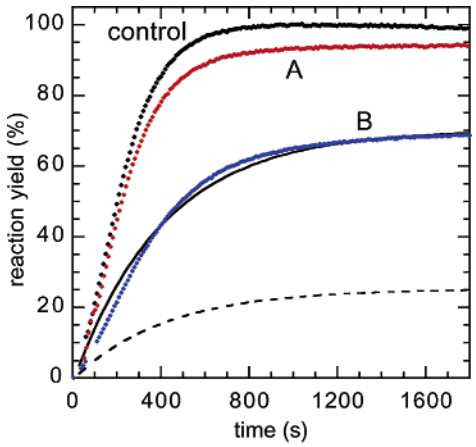

Figure 11. Kinetics of reaction of *MBTH* onto *LA* liposomes, in the presence or absence of *RGDH*. The fluorescence intensity of a suspension of *LA* containing liposomes (0.3 g/L lipids, accessible *LA* 10 μM) at pH 4.6 and 25 °C was recorded over time after addition of *MBTH* 1 mM (control), *MBTH* 1 mM + *RGDH* 1 mM (A), or *MBTH* 400 μM + *RGDH* 2 mM (B). the continuous line is the best fit of eq 11 to data B; the dashed line is the corresponding calculated course of reaction of *LA* with *RGDH*.

LA onion vectors incubated with *RGDH* (2393.6 [M + H^+], 2415.5 [M + Na^+], exact mass 2393). Unreacted *LA* was present in *LA* onion vectors incubated with or without *RGDH* (1296.0 [M + Na^+], exact mass 1272.5), as expected as only 10% of *LA* was accessible to reaction. Trace amounts of *RGDH* were detected only on control onion vectors incubated with *RGDH* (1138.7 [M + H^+], exact mass 1138), showing a weak adsorption of *RGDH* onto lipid membranes.

The reactivity of *RGDH* and *MBTH* were close as their reaction rate *k* in solution were similar. Taking into account its lower acidity ($pK'_a = 6.45$[33] compared to $pK'_a = 5.67$ for *MBTH*), *RGDH* was actually 2 times more reactive than *MBTH* at pH 4.6. This higher reactivity was correlated with a 100 times higher equilibrium constant *K* for *RGDH*: the stability of the *RGDH* α-oxohydrazone at nanomolar concentrations place it high above previously described hydrazones, whose stability do not exceed the micromolar range.[26,24]

On the other hand, the presence of lipid colloids induced no such acceleration effect on the reaction of *RGDH* as that observed with *MBTH*. This can be explained since *RGDH* is more hydrophilic than *MBTH* and should not show significant affinity for lipidic surfaces. However, as pointed out above, immobilizing the aldehyde reagent onto colloids should decrease the reaction rate because of its slower motion in the reaction medium. The similar reaction rates in solution and onto liposomes are indicative of a very weak adsorption of *RGDH* onto lipid bilayers, as confirmed by mass spectroscopy.

3.9. In Vitro Association of Targeted Vectors to Endothelial Cells. *RGDH* was designed to mediate association of *RGDH* grafted onion vectors to cells with active integrin receptors such as endothelial or bone marrow cells. The RGD ligand included in *RGDH* was chosen as the hexapeptide GRGDSP, which is the sequence of fibronectin recognized by integrins.[34] *RGDH* also included a hydrophilic spacer for grafting on different kinds of lipid aldehydes.[19] The spacer ensured a minimum distance to the surface of the onion vectors, as it has

(33) Bonnet, D.; Ollivier, N.; Gras-Masse, H.; Melnyk, O. *J. Org. Chem.* **2001**, *66*, 443−449.
(34) Ruoslahti, E. *Annu. Rev. Cell Dev. Biol.* **1996**, *12*, 697−715.

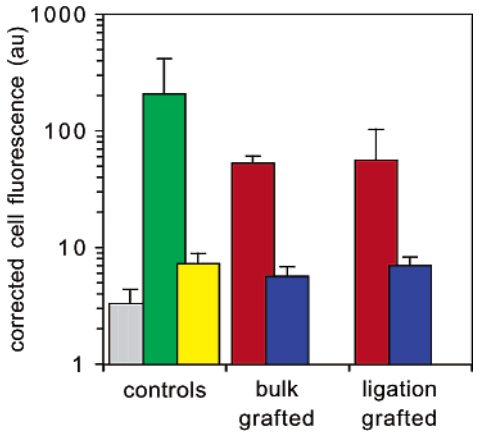

Figure 12. Corrected average fluorescence of live EAhy-926 cells incubated with onion vectors (0.5 g/L lipids) for 4 h at 37 °C (two independent experiments); gray bar: neutral control vectors; green bar: cationic vectors; yellow bars: non grafted *LA* vectors; red bars: RGD grafted vectors; blue bars: RGE grafted vectors. Onion vectors grafted by ligation of *RGDH* and *RGEH* (ligation grafted) are compared to vectors labeled with lipid−ligands *LRGD* and *LRGE* as in ref 14 (bulk labeled).

been shown that recognition of grafted RGD peptides by their cell receptors was inhibited if the ligands are too close to their support.[35] During the synthesis, the hydrazine moiety was provided by coupling of hydrazinoacetic acid as described by Bonnet et al.[17] As a control, we also prepared an RGE containing hydrazinoacetyl peptide *RGEH*, which differs from *RGDH* only in the replacement of the aspartate residue by a glutamate.

The vectors were prepared in the optimal conditions determined above, and their cell targeting efficiency was assessed in vitro using a previously described protocol.[14] Briefly, a fluorescent dye, calcein, was incorporated into the onion vectors. Cultured cells from the endothelial cell line EAhy-926 were incubated over 4 h with onion vectors at 37 °C. Cells were thoroughly washed, and their fluorescence was measured by flow cytometry (Figure 12). The fluorescence due to calcein was corrected by the intrinsic fluorescence of each type of onion vector, measured independently. As in our previous work,[14] the adhesion ability of RGD onion vectors was compared to those of neutral and cationic onion vectors. The first showed no affinity, and the latter, high affinity for the cell surface (Figure 12, controls). Neutral onion vectors containing unreacted *LA* behaved mostly like control neutral onion vectors. RGD grafted onion vectors proved to associate strongly with EAhy-926 cells compared to those controls. Also, when the RGD ligand sequence was changed for a RGE sequence, the affinity of association to cells was lost, showing that interaction of RGD onion vectors with cells was mediated by molecular recognition of the grafted ligands by their receptors at the cell surface.

Onion vectors grafted using the α-oxohydrazone ligation strategy were compared to onion vectors containing presynthesized lipid−ligands *LRGD* and *LRGE* with the same RGD or RGE peptide.[14] Both types of grafted vectors were very similar in their behavior toward cells. The presence of α-oxohydrazone products or unreacted α-oxoaldehyde moieties had neither an inhibitory effect on binding nor a detectable cell toxicity.

(35) Kantlehner, M.; Finsinger, D.; Meyer, J.; Schaffner, P.; Jonczyk, A.; Diefenbach, B.; Nies, B.; Kessler, H. *Angew. Chem., Int. Ed.* **1999**, *38*, 560−562.

4. Discussion

4.1. α-Oxohydrazone: A Kinetically and Thermodynamically Enhanced Hydrazone. A highly hydrolyzable bond such as hydrazone was not an obvious ligation bond for use in physiological conditions: although the reaction had the advantages of producing no undesirable subproduct and being chemoselective, the known stability of hydrazone bonds was at most in the micromolar range. For controlled modification of our onion vectors, we required grafted ligands that would stay in place for the duration of the cell targeting process.

The mechanism deciphered by Sayer et al. for imine and hydrazone formation predicted a faster and more thermodynamically favorable reaction in the case of a strong nucleophile reacting with a highly electrophilic carbonyl.[22] This was the case of our reagents: the α-oxoaldehydes obtained by periodate oxidation of threonine or serine possess a strongly electron deprived carbonyl because of the attractive vicinal carbonyl and the nitrogen in β. On the other hand, peptide hydrazines obtained by the Bonnet method[17] are rendered even more nucleophilic by the vicinity of the electron rich carbon of the peptide backbone. In accordance with Sayer's model, our kinetic data from the model reaction showed a fast and stepwise mechanism for hydrazone formation. However, the measured rate constants were unexpected. The rate constants of uncatalyzed or base catalyzed steps were within the range of previously reported data, but the rate constants of acid catalyzed steps (steps 1, 3, and 5, Figures 3 and 4) were unexpectedly high. We assume that acid catalysis in those steps was additionally favored by the vicinal carbonyl which could chelate hydronium ions in close proximity to the reaction center.

Although the chemoselectivity was not inquired directly in this study, no competing reaction was observed with the usual reactive groups present in biological macromolecules. In particular, the intramolecular primary amine of the lysine residue in *WA* could have been a competitor to hydrazines for reaction with the aldehyde. But this was not observed because hydrazines are far stronger nucleophiles than amines, as was already shown for amidation reactions.[5] Similarly, the guanidinium group of the arginine residue in *RGDH* could have produced a stable intramolecular bond with the 1,2 dione in the α-oxoaldehyde moiety. No evidence of a competition of this reaction with the hydrazone formation was recorded, not surprisingly given the higher nucleophilicity and lower basicity of hydrazines. Furthermore, a ligation reaction was performed in saturated saccharose solution, and no competition from the sugar aldehydes was observed.

Not only the reaction kinetics was surprising but also the thermodynamics. Hydrazones of our model reagent *MBTH* already showed a stability as high as the best reported carbazones. The product of reaction of the peptide hydrazine *RGDH* with the peptide aldehyde *WA* proved even more stable with an equilibrium constant 2 orders of magnitude higher. Furthermore, even at lower concentrations, bond hydrolysis was very slow. Indeed, the hydrolysis rate constants estimated at pH 7.4 and 25 °C give for our ligation products half-lives of 23 to 800 days. Even at 37 °C, the half-lives should be long enough for grafted vectors to touch and attach to their cell target in vivo. Therefore, the α-oxohydrazone ligation strategy exceeded the expectations of high reactivity and high stability compared to

usual hydrazones and finally met the basic requirements for its use as a ligation for biological applications.

4.2. Further Enhancing the Stability Using Lipophilic Self-Assembly. We intended to use the α-oxohydrazone ligation in onion vector suspensions, which could affect the kinetics of the reaction and the stability of the bond. Therefore, effects of self-organized media on the reaction were still to be investigated. The hydrazone bond formation proved even faster when involving the mildly lipophilic *MBTH* and the lipophilic aldehyde *LA* trapped onto colloids. The increase in global reaction kinetics was not due to a catalysis by colloids (the activation energy rather increased in colloidal suspension) but to concentration inhomogeneity in the reaction medium. A pseudophase model could successfully be applied to our data not only for micellar media, for which it has mainly been developed,[36] but also for more complex colloids such as liposomes and onion vectors. In accordance with this model, the strong anisotropic concentration effects in those suspensions resulted also in an increase in the apparent stability of the hydrazone product.

Although this constructive lipophilic self-assembly was absent or very weak in the case of the ligation of our peptide ligand *RGDH*, we plan to take advantage of it in more refined designs. First, the ligation of large hydrophilic macromolecules onto lipidic vectors would be slowed by the larger size of the reagent. It could also be challenged by a displaced hydrophilic/lipophilic balance, more favorable to anchor solubilization in water thanks to the macromolecule rather than to fixation of the macromolecule onto the colloid.[37] Lipophilic self-assembly could be used here. For example, a short aliphatic chain could be provided to the macromolecule together with the hydrazine or α-oxoaldehyde moiety prior to grafting. Such modifications are now accessible even on recombinant proteins.[1,6] Autoassociation would also be of great interest in the formation of structured peptide loops at the surface of vectors: indeed it has been largely emphasized that prestructured peptide ligands have stronger affinities for their receptors.[38] Peptide loops could be easily produced in our ligation strategy by providing the peptide ligand with an aliphatic chain at the nongrafted end.

4.3. α-Oxohydrazone Ligation Proved Efficient on Cells in Vitro. In our cell association test, RGD onion vectors obtained with the α-oxohydrazone ligation had excellent targeting abilities compared to those of RGD onion vectors using no ligation. As the two types of vectors proved completely equivalent for their biological activity, vector modification by the ligation strategy was preferred as it had many advantages. First, it provided a means for ligand saving: whereas only 10% of the lipid−ligand incorporated into the bulk labeled onion vectors was actually displayed at the surface, all the ligands grafted onto ligation grafted onion vectors were available for recognition by cells. Here the ligation was achieved using a 2-fold excess of ligands to increase the rate of reaction but could have been done in stoichiometric conditions if allowed to react overnight. Second, as a consequence, problems of chemical incompatibility or mutual exclusion inside the onion vector between the ligand and the encapsulated active compound would be avoided. Third, ligands to graft would be a lot more variable because hydrazinoacetyl peptides are a lot easier to synthesize than lipid−ligands. Fourth, the ligation strategy would allow more complex surface modifications, like the concurrent grafting of several ligands at the same time. Finally, let us note that no cytotoxicity was observed, either for α-oxoaldehyde onion vectors which had not been ligated or by ligation grafted onion vectors.

(36) Lopez-Cornejo, P.; Perez, P.; Garcia, F.; de la Vega, R.; Sanchez, F. *J. Am. Chem. Soc.* **2002**, *124*, 5154−5164.
(37) Silvius, J. R.; Zuckermann, M. J. *Biochemistry* **1993**, *32*, 3153−3161.
(38) Thorpe, D. S.; Yeoman, H.; Chan, A. W. E.; Krchnak, V.; Lebl, M.; Felder, S. *Biochem. Biophys. Res. Commun.* **1999**, *256*, 537−541.

5. Conclusion

Our study on a model reaction of the kinetics and thermodynamics of α-oxohydrazone bond formation has shown that this reaction is an efficient ligation reaction. Submicromolar stability was achieved as well as half-lives of several weeks for ligation products in solution. When the ligation was performed in self-organized media, the kinetics and stability were enhanced thanks to autoassociation of the reagents. The ligation of ligands onto colloidal biological vectors can therefore prove more efficient and favorable than the ligation of soluble molecules. Those results could be extended to the reagents of interest, namely targeting peptides grafted as molecular addresses onto onion vectors. At last, specific cell association tests proved the biological relevance of this approach.

Our efforts now turn to the use of this ligation strategy for grafting more complex ligands. The high chemical specificity of α-oxoaldehyde/hydrazine reactivity allows us to use this ligation for any kind of protein, glycosylated or not.[6] Hydrolysis of the ligation bond was both unfavorable and very slow; but, as has been developed for disulfide coupling,[2] it could also be tuned for directed hydrolysis in endosomes, where the acidic pH catalyzes hydrolysis. Finally, the ligation of macromolecules could be enhanced in terms of kinetics as well as stability by taking advantage of the lipophilic autoassociation process we have observed in our model reaction. Preparation of peptide loops on lipidic colloids are currently under study.

Acknowledgment. We would like to thank O. Melnyk for his advice; N. Ollivier for providing the *WA* reagent; K. Torrecillas for help in the chemical characterization; J. Thimonier and J. Barbet for AFM experiments; H. Drobecq for the mass spectroscopy analysis; and S. François, B. Delord, and A. Février for their help in cell culture and experiments. This work was supported by the CNRS and the University of Bordeaux Sciences and Technology.

Supporting Information Available: Preparation of compounds *RGDH*, *RGEH*, *LRGD*, and *LRGE*. This material is available free of charge via the Internet at http://pubs.acs.org.

JA0370746